Turkish Journal of Electrical Engineering & Computer Sciences

http://journals.tubitak.gov.tr/elektrik/

Research Article

Turk J Elec Eng & Comp Sci
(2015) 23: 539 – 547

doi:10.3906/elk-1301-51

The detailed analysis of rate equation roots of BH-laser diode using Volterra series

Remzi YILDIRIM[1], **Ahmet KARAARSLAN**[2,*]

[1]Department of Electrical and Electronics Engineering, Faculty of Engineering and Natural Sciences, Yıldırım Beyazıt University, Ankara, Turkey

[2]Department of Electrical Engineering, Faculty of Engineering, Afyon Kocatepe University, Afyonkarahisar, Turkey

Received: 09.01.2013 • **Accepted:** 15.04.2013 • **Published Online:** 23.02.2015 • **Printed:** 20.03.2015

Abstract: In this study, the rate equation analysis of a BH-laser diode was performed for output carrier density (N_o) using the zero-degree solution of the Volterra series. The carrier rate equation of the laser diode was analyzed in terms of input carrier density (N_i) and output carrier density modeling ($N_i - N_o$), with respect to the DC current (I_o). The polynomial root, which is obtained from the zero-degree solution (N_o) and limit values of I_o, was found. For the linear operation of the laser diode, the range of I_o current was also determined using a linearization approach and the maximum value of N_o.

Key words: Laser diode, rate equations, Volterra series, nonlinear analysis

1. Introduction

A semiconductor laser diode is necessary and one of the most important devices of commercial fiberoptic telecommunications and data transmission systems. It has 3 main characteristics [1–9]: gain [10–17], refractive index change [18,19], and alpha parameter [20–23]. This study is closely related to the gain, which also affects the other characteristic quantities.

The other elements used in the communication or data transmission system are selected according to the optical output power that is produced by the diode laser. The state of the optical output power is specifically important due to the effects of intermodulation distortion on applications and subcarrier systems. One especially important feature is the effect and fluctuation of optical power, which is more evident and greater when a low DC supply current (I_o) is applied [24–31]. As the amount of power increases to a certain level, the power fluctuation may be reduced significantly. However, it cannot be eliminated completely. Some of the techniques that are used to reduce fluctuations are optical, electronic or optoelectronic feedbacks, or a combination of these.

2. The basic rate equations of laser diodes

In this study, the kernels of the Volterra series (H1, H2, and H3) are analyzed. The equations of Hassine et al. [32] are approximations for the exact rate equations. We use the basic single-mode laser diode rate equations

*Correspondence: akaraarslan@aku.edu.tr

given by Hassine et al [32] to develop our model:

$$\frac{dp(t)}{dt} = \Gamma A\left[n(t) - N_{tr}\right]\left[1 - \hat{\varepsilon}p(t)\right]p(t) - \frac{1}{\tau_p}p(t) + \frac{\beta\Gamma}{\tau_n}n(t), \tag{1}$$

$$\frac{dn(t)}{dt} = \frac{1}{q}I(t) - \frac{1}{\tau_n}n(t) - \Gamma A\left[n(t) - N_{tr}\right]\left[1 - \hat{\varepsilon}p(t)\right]p(t), \tag{2}$$

in which $p(t)$ is the photon population number and $n(t)$ is the charge carrier population number inside the laser diode active region. The other laser diode parameters are given in the Table.

Table. Laser diode parameters.

Γ	Confinement factor	0.3
A	Gain coefficient	$1.83 \times 10^4\,\mathrm{s}^{-1}$
N_{tr}	Carrier density at transparency	10^7
τ_p	Photon lifetime	$1.6 \times 10^{-12}\,\mathrm{s}$
τ_n	Carrier recombination lifetime	$2.2 \times 10^{-9}\,\mathrm{s}$
β	Spontaneous emission fraction	10^{-4}
$I(t)$	Total current	
q	Electron charge	$1.6 \times 10^{-19}\,\mathrm{C}$
$\hat{\varepsilon}$	Dimensionless gain factor in which V is the active region volume	$\hat{\varepsilon} = \varepsilon/V = 10^{-6}$

3. The zero-order solution

We first determine N_o and P_o. We obtain:

$$P_o = \frac{\tau_p}{q}I_o + \frac{\tau_p}{\tau_n}\left[\beta\Gamma - 1\right]N_o. \tag{3}$$

Substituting this expression for P_o, we obtain the cubic polynomial

$$N_o^3 + N_o^2 R_{2N} + N_o R_{1N} + R_{oN} = 0, \tag{4}$$

in which

$$R_{2N} = -\left[N_{tr} + \frac{\tau_n}{\tau_p\hat{\varepsilon}\left(\beta\Gamma - 1\right)}\right] + \frac{2\tau_n}{q\left(\beta\Gamma - 1\right)}I_o,$$

$$R_{1N} = -\frac{1 - \Gamma A N_{tr}\tau_p\left(\beta\Gamma - 1\right)}{\Gamma A\hat{\varepsilon}\tau_p\left(\beta\Gamma - 1\right)^2}\frac{\tau_n}{\tau_p} + \frac{2\hat{\varepsilon}N_{tr}\tau_p\left(\beta\Gamma - 1\right) + \tau_n}{q\hat{\varepsilon}\left(\beta\Gamma - 1\right)^2}\frac{\tau_n}{\tau_p}I_o + \left[\frac{\tau_n}{q\left(\beta\Gamma - 1\right)}\right]^2 I_o^2,$$

and

$$R_{oN} = \frac{1 + \tau_p\beta\Gamma N_{tr}}{q\Gamma A\hat{\varepsilon}\left(\beta\Gamma - 1\right)^2}\left(\frac{\tau_n}{\tau_p}\right)^2 I_o - \left[\frac{\tau_n}{q\left(\beta\Gamma - 1\right)}\right]^2 N_{tr}I_o^2. \tag{5}$$

Comprehensive analysis of this solution and the Volterra series is made in [24,33–36]. The roots curves that are obtained from the zero-degree equation (Eq. (4)) are given below. The first root curve is shown in Figures 1 and 2. Figure 1 illustrates the $I_o - N_o$ (output current-carrier density) increase. This curve corresponding to I_o does not increase linearly with the increase in N_o. The characteristics of N_o between current values of 0 and

37 mA are decreasing, and at 37 mA it is approaching zero. We observe a cycle between 37 mA and 161 mA; it increases for I_o values greater than 37 mA until a local minimum value, after which it declines and approaches zero value at 161 mA. We then observe a nonlinear increase between 161 and 300 mA current values.

Figure 2 shows the first root of N_i and N_o variation. The value of N_i saturates approximately at $N_i = 1 \times 10^{29}, N_o = 2.1 \times 10^{27}$. When the I_o current is increased, the value of N_i also increases. However, a nonlinear decrease in N_o occurs after the saturation point. dNo/dNi varies in a nonlinear manner.

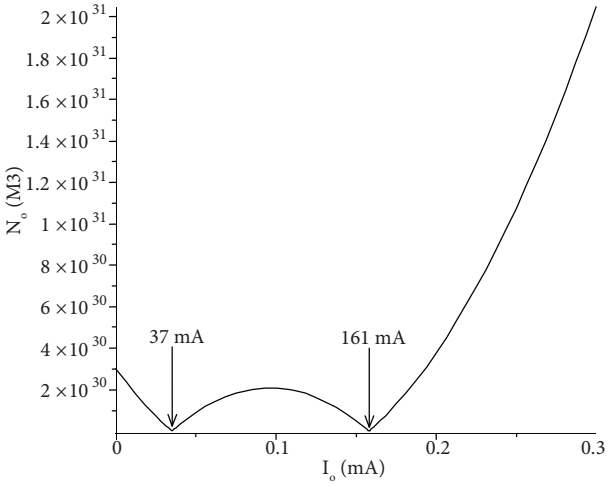

Figure 1. First root curve of I_o and N_o.

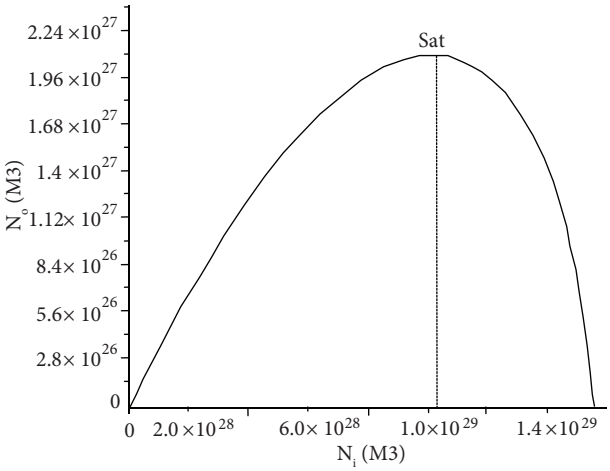

Figure 2. First root of N_i-N_0 variation.

The second root of $N_i - N_o$ variation is seen in Figure 3. The overall structure of injected carrier density and current change is in the third-level type of deviation point. In general, this type is the unique singular point of origin.

The third root of $I_o - N_o$ variation is seen in Figure 4. This corresponds to the increase in I_o current between 0 and 37 mA, where the reduction of N_o occurs. This reduction is a low-order one that can be accepted as linear with negligible error.

When the I_o current increases from 37 mA to 180 mA, N_o increases nonlinearly. dN_o/dI_o displays the nonlinear variation. Therefore, the linear increase in variation cannot be obtained as a function of N_o.

The relationship between $N_i - N_o$ curves is shown in Figure 5. This curve was obtained using the I_o current from 15 to 45 mA. The curve can be considered linear with negligible error for approximately $\pm 1.5 \times 10^{28}$ M^3 values of N_i. The value of $\pm 1.5 \times 10^{28}$ M^3 can be used in real applications. Carrier density displays nonlinear conductance characteristics [35].

Figure 5 shows a nonlinear conductance curve of current-voltage curve type. The type of nonlinear conductance equation is given as $i_{\max} tgh\,[(g\nu)/(i_{\max})]$. This equation can be taken as an electrical equivalent circuit of the laser diode. When this arrangement is completed, the maximum value of I_o that is feasible in the linear region can be found. The variation of dN_o/dN_i shows the same slope or gain in the limited region. It displays linear characteristics disregarding small amount of errors in this region.

The overall structure of $N_i - N_o$ root variation was also obtained as in Figure 6. The structure of the roots is a curve that rotates counter-clockwise. The carrier density (N_o) is also a parabolic curve. The effect of neither the saturation current nor the noise can be seen directly in the employed equations. The N_i value decreases after reaching a maximum value, while N_o value increases. Although we acknowledge this theoretically,

we do not think that this is acceptable for practical applications. However, in theory, the production of N_i depends on the input current I_o, and therefore this case is a contradiction. According to these curves, the rotation points of 1, 2, and 3 roots can be accepted as the largest values of N_i. The peak values of the roots are obtained as follows:

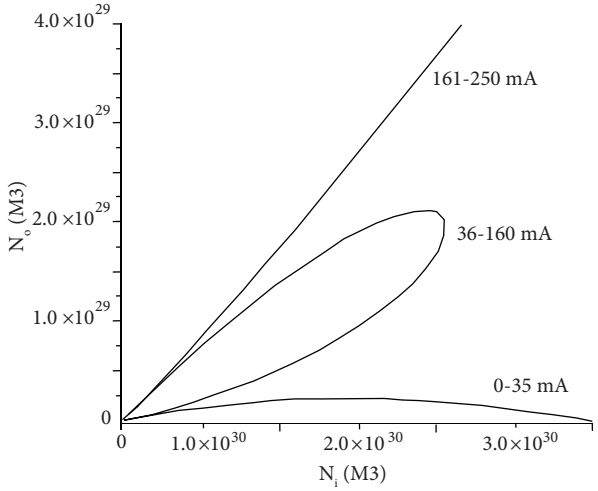

Figure 3. Second root of N_i-N_o variation.

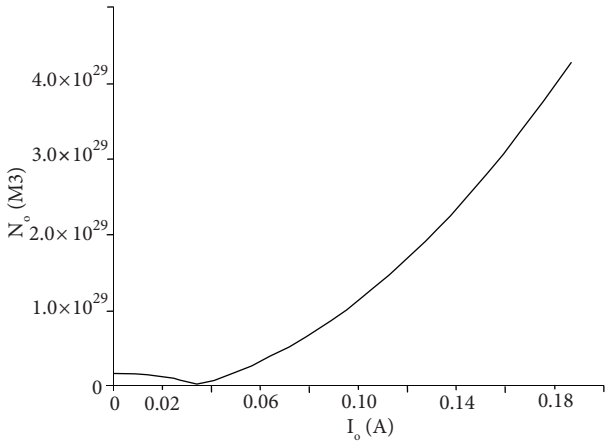

Figure 4. Third root of $I_o - N_o$ variation.

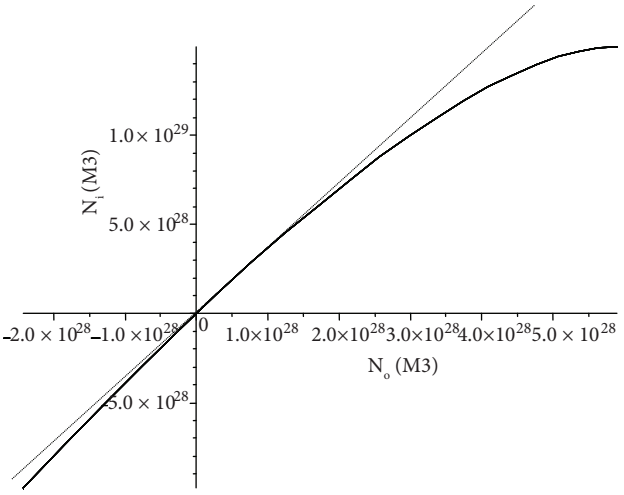

Figure 5. Third root of N_i-N_o (14–50 mA) variation.

$1 \rightarrow Ni = 0.65x10^{32} \rightarrow No = 1.6x10^{32}$, $\quad 2 \rightarrow Ni = 7.5.x0^{32} \rightarrow No = 1.3x10^{33}$, and

$3 \rightarrow Ni = 2.5x10^{32} \rightarrow No = 3x10^{32}$.

In the descending order of 1, 3, and 2, the rate of increase or the angle of the gradient of N_i describes a straight line. However, the decrease in N_i versus increasing N_o is observed in the results for the roots of 1, 2, and 3. This is not physically possible. We acknowledge these turning points as the maximum value of N_i. Accordingly, the photon output is also reduced. This corresponds to the maximum carrier density at a point of saturation current.

Under these conditions, the maximum value that may be acknowledged is $N_o = 1.3 \times 10^{33}$ M^3. All kinds of noises are the results of other effects in this equation. When we remove the loss terms from this theoretical multiplication, the real value of N_o can be obtained. As a function of real N_o or gain, the photon density at the output can be obtained. Accordingly, N_o is greater than N_i at the input. Under normal circumstances, this cannot be correct. These results are directly related to the photon density, gain, and optical output power of the laser diode. $G = \Gamma g \nu_g$ is defined as the linear net gain [37–42]. The first practical solution of these processes to increase this gain is selecting a material with high gain when manufacturing the laser diode. The second solution is to boost the confinement factor (Γ) or decrease the group velocity (ν_g). Certainly, optimum results can be obtained if all of these solutions are applied altogether. However, in practice, this is not always feasible. The largest value of the roots has been identified as $N_i = 7.5 \times 10^{32}$ M^3. This value is the peak or the return value of the parabola. The rate values of N_i/N_o and N_o/N_i correspond to 0.576 and 1.733, respectively. This ratio is obtained theoretically with no loss as a result of the 3 roots, which are derived from Eq. (4). $N_p + \Delta N_p = N p e^{g \Delta z}$ is defined as the ultimate density. The parameter ΔN_p can be set as $N_p g \nu_g \Delta t$. This change is defined by $\left(\frac{dN_p}{dt}\right) = R_{st} = \frac{\Delta Np}{\Delta t} = \nu_g g N_p$ or $\frac{dN}{dt} = \frac{\eta_i I}{qV} - \frac{N}{\tau} - \nu_g g N_p$. Depending on the carrier density, the characteristics of optical power can be changed by $V/V_p(\Gamma)$ [37–42].

Gain is defined as a function of the carrier $g \approx \alpha(N - N_{tr})$. α expression in the differential gain is defined as the $\partial g/\partial N$. From the values of electron density (V) and photon density (V_p), the electron-photon overlap factor can be given as V/V_p. This confinement factor (Γ) is defined in [37–42]. According to these definitions, the value of $N_o/N_i = 1.733$ is not correct. Depending on the previous study, the calculation of values of N and P was completed related to the I_o current. Thus, the second root is used as an appropriate root [24]. The other 2 roots are not suitable for N and P values. The lack of solution after 1250 mA in the present study is displayed. This study supports our previous works.

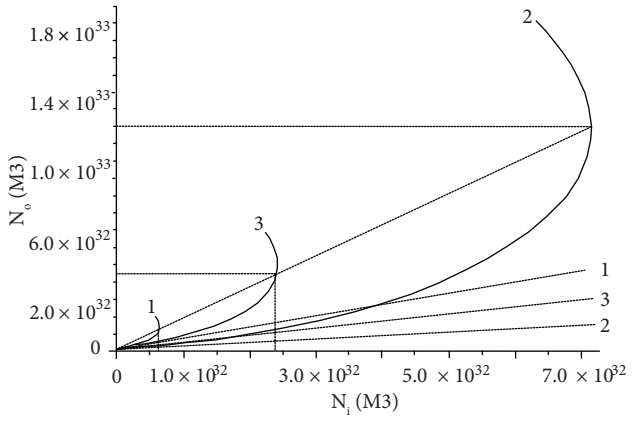

Figure 6. Overall structure of $N_i - N_o$ root variation.

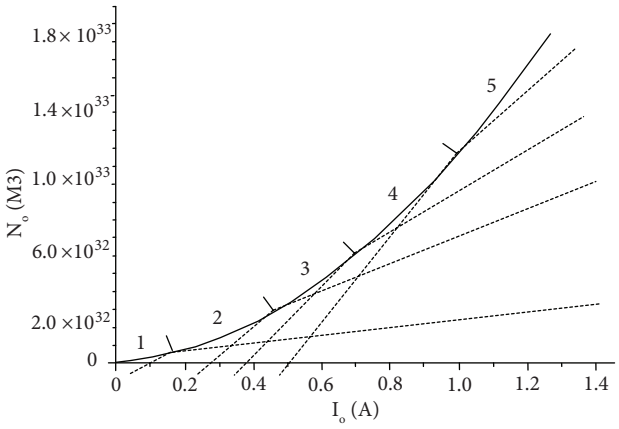

Figure 7. Total $I_o - N_o$ output and piecewise linear approach.

I_o currents versus the total carrier density are obtained in Figure 7. The value of N_o that is obtained from the zero-order solution can be evaluated by the gain according to the partial linearity. These regions are divided into 5 categories. The slope of the straight lines can be given as:

1st region: This region corresponds to slope (m) tg = 9.7°.

2nd region: This region corresponds to slope (m) tg = 24.3°.

3rd region: This region corresponds to slope (m) tg = 37.87°.

4th region: This region corresponds to slope (m) tg = 46.87°.

5th region: This region corresponds to slope (m) tg = 54.70°.

The region of the largest or the most rapid variation of dN_o/dI_o is the 5th region. However, the 5th region corresponds to the $I_{th} = 13.8$ mA of laser diode, and the I_o current is equal to 1250 mA. This current is quite large for the laser diodes. Therefore, it is theoretically probable but not practically possible. In addition, we showed that Eqs. (1) and (2) were unresolved after 1250 mA in previous studies [25]. In this case, the 1st and 2nd regions are appropriate for practical applications of the laser diode. Slope angles of these regions are 9.7° and 24.30°, respectively. Region 2 has more gain than others in the nonlinear curve that is obtained from Figure 7. Thus, the N_o value will be bigger in than other regions. These values of N_i, N_o, and rate are 5×10^{32} M^3, 3.5×10^{32} M^3, and $N_o/N_i = 3.5/5 = 0.7$, respectively. If the other losses are subtracted from these values, the N_o/N_i ratio falls to much lower values. Taking into account that the confinement factor ($\Gamma = V/V_p$) is approximately 0.3 in practice, the N_o/N_i ratio is only effective for a very small part of the photon production [37–42]. The best linear region is region 1, in which the I_o current is below 100 mA. Region 1 can be considered as the most linear part of the optical output power. I_o injection current with maximum gain is 67.55 mA and 24–30.50 mA for the best linear region, as stated in [30]. There is a direct and indirect relationship between dP_o/dI_o and dN_o/dI_o slopes in the piecewise linear approach.

The output power and current of the CW laser diode characteristics obtained from the experimental results are given in Figure 8. There is a close relationship between the optical output power and the carrier density. When the absolute gain $^{dp(t)}/_{dt} = (G - \gamma) P + R_{sp}$ increases, the optical output power increases, too [39,40]. The turning point of the power-current curve corresponds to the maximum output power. After reaching the maximum value of power, the gain and the output power decrease. Optical output power is limited by limiting the gain increase. The optical output power is decreased due to the decreasing gain. This situation indirectly affects the state of N_o carrier density. The power-current curve that is obtained via experimentation is also given in Figure 9.

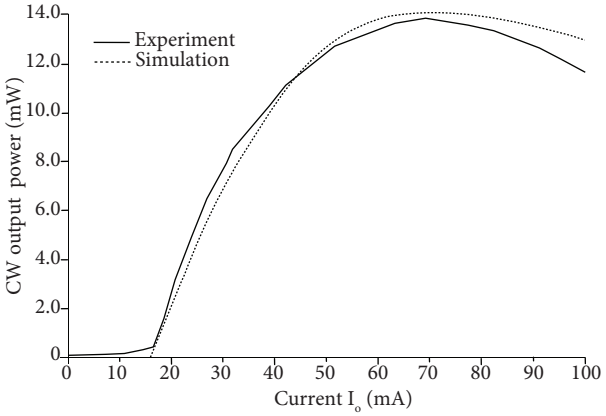

Figure 8. Optical output power versus current (I_o) of CW laser diode.

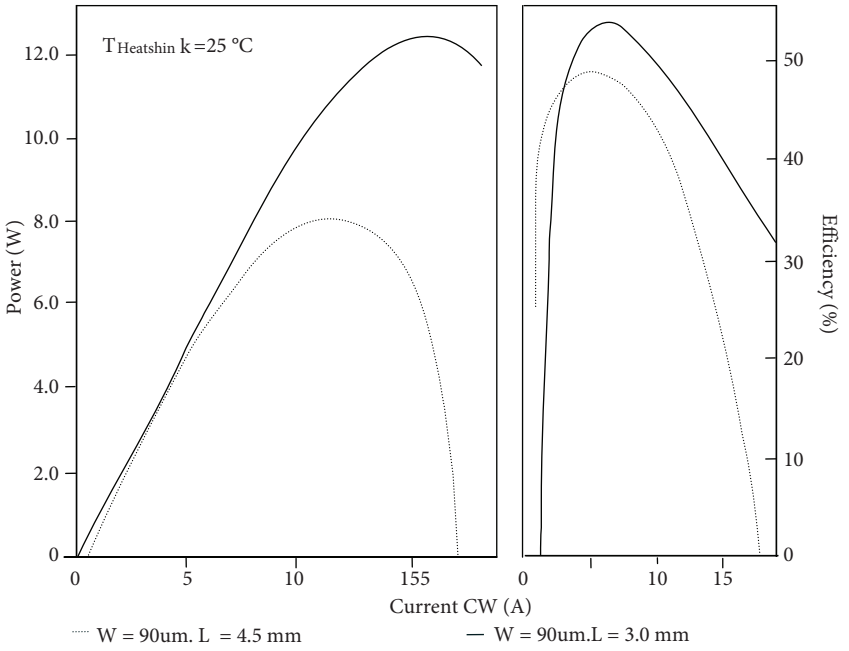

Figure 9. CW laser diode characteristics obtained in [43].

4. Conclusion

In this study, an analysis of the carrier density (N) rate equation of laser diodes was performed. In this analysis, the results obtained from the zero-order solutions are:

1. Root change is not linear.

2. Noise effects are not observed directly.

3. Although there is no saturation current in the expression, maxima are found in the analysis of the root equations.

The following results are found as shown in Figure 6:

for N_o ,

$1 \rightarrow 20\log 10(1x10^{32}) = 640\,dB$, $3 \rightarrow 20\log 10(4.5x10^{32}) = 653\,dB$, and $2 \rightarrow 20\log 10(1.3x10^{33}) = 662\,dB$;

for N_i,

$1 \rightarrow 20\log 10(0.75x10^{32}) = 637\,dB$, $3 \rightarrow 20\log 10(2.5x10^{32}) = 647\,dB$, and $2 \rightarrow 20\log 10(7.3x10^{32}) = 657\,dB$.

Temperature dependencies of the variables used in the equations of this study are not known. In this aspect, this is a shortcoming. However, in this case, the real photon (P) output was obtained. In addition, we think that every noise term should be taken into account. Theoretically, the laser diode rate equation has a solution as $I_o \rightarrow \infty$. However, root variations for I_o have a solution in the limited area. In that case, the results are not suitable for practical applications in the calculation of the carrier density. The conclusion that the optical output power is affected by carrier density is important for practical applications. The consistency of the experimental result with the theoretical results proves the applicability of the proposed study.

In future studies, the rate equations must be rearranged for infinitive real solutions of I_o. These equations should be included in various arrangements depending on noises, temperature of variables, saturation, and cutting conditions. In this case, the application will be closer to the obtained real results.

References

[1] Celebi FV. A proposed CAD model based on amplified spontaneous emission spectroscopy. J Optoelectron Adv M 2005; 7: 1573–1579.

[2] Celebi FV, Yucel M, Goktas HH. Fuzzy logic based device to implement a single CAD model for a laser diode based on characteristic quantities. Optik 2012; 123: 471–474.

[3] Celebi FV, Dalkiran I, Danisman K. Injection level dependence of the gain, refractive index variation, and alpha (α) parameter in broad-area InGaAs deep quantum-well lasers. Optik 2006; 117: 511–515.

[4] Celebi FV, Altindag T, Yildirim R, Gökrem L. Semiconductor laser modeling with ANFIS. In: International Conference on Application of Information and Communication Technologies. Baku, Azerbaijan: IEEE, 2009. pp. 1–4.

[5] Yucel M. Fuzzy logic-based automatic gain controller for EDFA. Microw Opt Techn Let 2011; 53: 2703–2705.

[6] Yucel M, Göktas HH. C band erbium doped fiber amplifier as a flat gain optical amplifier. In: IEEE 16th Signal Processing, Communication and Applications Conference. Aydın, Turkey: IEEE, 2008.

[7] Yücel M, Göktaş HH. Design of gain flattened ultra-wideband hybrid optical amplifier. J Fac Eng Arch Gazi Univ 2007; 22: 863–868 (in Turkish with English abstract).

[8] Yücel M, Göktaş HH, Özkaraca O. Temperature dependence of noise figure in the erbium doped fiber amplifier. J Fac Eng Arch Gazi Univ 2010; 25: 635–641 (in Turkish with English abstract).

[9] Yigit S, Tugrul B, Celebi FV. A complete CAD model for type-I quantum cascade lasers with the use of artificial bee colony algorithm. Journal of Artificial Intelligence 2012; 5: 76–84.

[10] Yamada M, Suematsu Y. Analysis of gain suppression in undoped injection-lasers. J Appl Phys 1981; 52: 2653–2664.

[11] Celebi FV, Yücel M, Yigit S. Optical gain modelling in type I and type II quantum cascade lasers by using adaptive neuro-fuzzy inference system. In: IEEE 20th Signal Processing and Communications Applications Conference. Muğla, Turkey: IEEE, 2012.

[12] Yigit S, Eryigit R, Celebi FV. Optical gain model proposed with the use of artificial neural networks optimised by artificial bee colony algorithm. Optoelectron Adv Mat 2011; 5: 1026–1029.

[13] Yucel M, Goktas HH, Celebi FV. Temperature independent length optimization of L-band EDFAs providing flat gain. Optik 2011; 122: 872–876.

[14] Celebi FV, Altindag T. An accurate optical gain model using adaptive neurofuzzy inference system. Optoelectron Adv Mat 2009; 3: 975–977.

[15] Celebi FV. A different approach to gain computation in laser diodes with respect to different number of quantum-wells. Optik 2005; 116: 375–378.

[16] Yücel M, Göktas HH, Celebi FV. The effect of pump laser wavelength change on the temperature dependence of EDFA. In: IEEE 19th Signal Processing and Communications Applications Conference. Antalya, Turkey: IEEE, 2011. pp. 238–241.

[17] Çelebi FV, Yıldırım R. Distortion system theory of the two tone small signal input laser diode. J Fac Eng Arch Gazi Univ 2005; 20: 373–377 (in Turkish with English abstract).

[18] Celebi FV, Danisman K. A different approach for the computation of refractive index change in quantum-well diode lasers for different injection levels. P SPIE 2004; 61: 384–388.

[19] Wenzel H, Erbert G, Enders, PM. Improved theory of the refractive-index change in quantum-well lasers. Journal of Selected Topics in Quantum Electronics 1999; 5: 637–642.

[20] Henry CH. Theory of the linewidth of semiconductor-lasers. Journal Of Quantum Electronics 1982; 18: 259–264.

[21] Çelebi FV. Modeling of the linewidth enhancement factors of the narrow and wide GaAs well semiconductor lasers. J Fac Eng Arch Gazi Univ 2006; 21: 161–166 (in Turkish with English abstract).

[22] Celebi FV, Danisman K. Neural estimator to determine alpha parameter in terms of quantum-well number. Opt Laser Technol 2005; 37: 281–285.

[23] Sagiroglu S, Celebi FV, Danisman K. Modelling of the linewidth enhancement factor with the use of radial basis function network. AEU-Arch Elektron Ub 2002; 56: 51–54.

[24] Schetzen M, Yildirim R. System theory of the single-mode laser-diode. Optic Communication 2003; 219: 341–350.

[25] Yildirim R, Schetzen M. Applications of the single-mode laser-diode system theory. Optic Communication 2003; 219: 351–355.

[26] Aydin E, Yildirim R. Optimization applications of the single-mode laser diode system using genetic algorithm. Optics and Laser Engineering 2004; 42: 41–46.

[27] Schetzen M, Yildirim R, Celebi FV. Intermodulation distortion of the single-mode laser diode. Appl Phys B-Lasers O 2008; 93: 837–847.

[28] Yildirim R, Yavuzcan HG, Celebi FV, Gökrem L. Temperature dependent Rolletti stability analysis of GaN HEMT. Optoelectron Adv Mat 2009; 3: 781–786.

[29] Yıldırım R, Çelebi FV. The computation of the angle between the gain and photon population by geometrical approach. J Fac Eng Arch Gazi Univ 2009; 24: 709–714 (in Turkish with English abstract).

[30] Yıldırım R, Çelebi FV. Harmonic amplitude control in laser diodes with non-linear feedback. J Fac Eng Arch Gazi Univ 2010; 25: 163–170.

[31] Cohen G. Thermal impedance measurements of junction-down mounted single-side contact laser diodes. Elec Comp C 2004; 1: 807–812.

[32] Hassine L, Toffano Z, Lamnabhi-Lagarrigue F, Destrez A, Joindot I. Volterra functional series expansions for noise in semiconductor lasers. IEEE J Quantum Elect 1994; 30: 2534–2546.

[33] Tankiz, S, Celebi FV, Yildirim R. Computer-aided design model for a quantum-cascade laser. IET Circ Device Syst 2011; 5: 143–147.

[34] Bussgang JJ, Ehrman L. Analysis of nonlinear systems with multiple inputs. P IEEE 1974; 62: 1088–1119.

[35] Weiner DD, Spina JE. Sinusoidal Analysis and Modeling of Weakly Nonlinear Circuits. New York, NY, USA: Van Nostrand Reinhold, 1980.

[36] Rugh WJ. Nonlinear System Theory. Baltimore, MD, USA: Johns Hopkins University Press, 1981.

[37] Petermann K. Laser Diode Modulation and Noise. Boston, MA, USA: Kluwer Academic, 1988.

[38] Yariv A. Optical Electronics in Modern Communications. 5th ed. New York, NY, USA: Oxford University Press, 1997.

[39] Agrawal GP, Dutta NK. Long-Wavelength Semiconductor Lasers. New York, NY, USA: Van Nostrand Reinhold, 1986.

[40] Agrawal GP, Dutta NK. Semiconductor Lasers. New York, NY, USA: Van Nostrand Reinhold, 1993.

[41] Lang R, Kobayashi K. External optical feedback effects on semiconductor injection laser properties. Quantum Electron+ 1980; 16: 347–355.

[42] Coldren LA, Corzine SW. Diode lasers and photonic integrated circuits. Microwave and Optical Engineering 2003; 2: 87–121.

[43] Gapontsev V, Moshegov N, Trubenko P, Komissarov A, Berishev I, Raisky O, Strougov N, Chuyanov V, Kuang G, Maksimov O et al. High-brightness fiber coupled pumps. P SPIE 2005; 7198: 71980O.